Microstructural and current-voltage characteristics in Mo/HfO_2/n-Si based metal-insulator-semiconductor (MIS) Schottky diodes using different methods

V. Manjunath[1]*, G. Nagaraju[4], M. Vani[2], S. Dastagiri[3], M. V. Lakshmaiah[3]**

[1]Department of Physics, Sri Padmavati Mahila Viswavidyalayam, Tirupati, A.P., India
[2]Department of Applied Micro biology, Sri Padmavati Mahila Visvavidyalayam, A.P, India-517 502
[3]Department of Physics, Sri Krishnadevaraya University, Anantapuramu, A.P, India
[4]Department of Physics (Electronics), Sri Venkateswara University, Tirupati, A.P, India-517 502

E-mail address: drvmanju18@gmail.com (***Dr. V. Manjunath***) *Corresponding author.

E-mail address: drmvl2009@gmail.com (***M. V.Lakshmaiah***) *Co-Corresponding author.

ABSTRACT

This paper investigates the effect of hafnium dioxide (HfO_2) thin film as interlayer between the Mo and n-Si semiconductor on the electrical characteristics of the Mo/n-Si Schottky diode (SD). The X-ray photoelectron spectroscopy (XPS) and X-ray diffraction (XRD) results confirmed that HfO_2 films were formed on the n-Si semiconductors. The image from SEM displays that the deposited HfO_2 thin film had a uniform appearance good smoothness of the surface. The smooth surfaces of the insulating layer strongly influence the electrical properties of the diode. The electrical properties of the Mo/HfO_2/n-Si metal/insulator/semiconductor (MIS) diode were obtained via current-voltage (I-V) measurements in the voltage range from −3 V to +3 V at room temperature. A better rectifying ability and a reduced reverse leakage current were demonstrated by the MIS diode. The MIS dide's barrier height (Φ_b) and ideality factor value were calculated to be 0.85 eV and 1.21, respectively. The MIS diode was able to achieve a higher b, which allowed the HfO_2 interlayer to change Φ_b. The calculated Φ_b values from the I-V, Hernandez, Cheung, and Norde approaches were comparable to one another, demonstrating their validity and consistency. The MIS diode's forward bias log (I) - log (V) curve demonstrated that it was ohmic in low-voltage regimes and that conduction was space-charge-limited in high-voltage regimes. However, for the MIS diode, the Poole-Frenkel and Schottky emissions are the

dominant current conduction mechanisms in the lower and higher bias regions. These outcomes indicate that the HfO_2 film can be chosen as dielectric materials in the construction of MIS devices.

Keywords: High-k HfO_2, n-type Si, MIS diode, structural and electrical properties.

1. Introduction:

Schottky diode (SDs) is such a helpful component since it can be utilised as a switch in radio frequency applications and as a rectifier in power applications. Studies on the characteristics and uses of these devices have been extensively studied [1-7]. In these SDs, it is important to understand the nature of the transmission mechanism and interface homogeneity [3]. The interfacial layer fabrication procedures and the preparation conditions are two of the most important elements determining the physical and electrical properties of Schottky diode devices. If an interface layer exists between the top contact and semiconductor, it may be prompted to change a number of diode features [8].

Various metal oxides such as SiO_2, V_2O_5, Ga_2O_3, TaO_2, TiO_2, ZrO_2, Ta_2O_5, Sm_2O_3, Al_2O_3 and HfO_2 [9-13] have been used as an interfacial layer for SDs. Among them, HfO_2 plays an important role in SDs. HfO_2 has attracted attention due to its chemical and good thermal stability [13], high dielectric constant (~25) [14], high refractive index and large band gap width (5.4 eV) and infrared bands and good transmittance in ultraviolet, making it a competitive candidate for Schottky devices, optical materials and resistive switching oxides [15–17]. Controlling the characteristics of the interlayer is therefore critical for improving the device performance level. For example, Al/HfO_2/p-Si (MIS) structures were created by Ozden et al. using the sol-gel process at three different annealing temperatures and insulating layer thicknesses. They demonstrated that as insulator layer thickness is increased, ideality factor (n) and interface state density (Nss) values increase [18]. Al/HfO_2/n-Si (SDs) were developed by Harishsenthil et al. using various HfO_2 substrate temperatures. They suggested

that the substrate temperatures had a significant impact on the diode characteristics [19]. By depositing ALD, Kaufmann et al. developed the insulating layers of HfO_2 and TiO_2 with thicknesses of 1, 2, and 4 nm. By adjusting the measurement temperature (297-373 K), current-voltage curves were derived from the diodes. For both dielectrics, thicker insulating layers result in larger n and lower SBH real values [20]. The hydrogen detection capabilities of a Pd/HfO_2/GaN-based MOS structure at varied hydrogen gas concentrations are studied by Chen et al. [15]. When exposed to 1% H_2/air gas at 300 K, the examined MOS structure displays a good hydrogen detecting response of 4.9×10^5 (139) under an applied forward- (reverse-) voltage of 0.5 V (-2 V). The Pt/HfO_2/n-GaN MIS structure underwent I-V characterization throughout a temperature range of 150 K to 370 K by Shetty et al. [12] in order to better understand the Pt/HfO_2/GaN interface. The BH increased (from 0.3 eV to 0.79 eV) and the ideality factor decreased (from 3.6 to 1.2) as the temperature increased from 150 K to 370 K. Both theoretical and practical researches have proven that the interface layer in MS devices has a considerable impact on the dielectric characteristics and other fundamental electrical parameters. Studying the electrical parameters that affect the effectiveness, stability, and dependability of the device is crucial.

Despite the potential benefits of HfO_2 thin films as a high-dielectric-index oxide interlayer, there are some research reports on the fabrication and electrical characterization of HfO_2/Si diodes using various metal contacts. To the best of our knowledge, no studies on the fabrication and characterization of molybdenum (Mo) as a Schottky electrode, aluminium (Al) as an ohmic contact, and HfO_2 as an insulating layer on n-type Silicon (Si) substrate to prepare MIS SDs have been published. In order to do this, radio frequency (RF) and direct current (DC) magnetron sputtering were used to fabricate the Mo/HfO_2/n-Si metal-insulator-semiconductor (MIS) type Schottky diode. The MIS diode, microstructural, morphological and electrical characteristics are therefore prepared and characterised. First, the

microstructural and morpological characteristics of the HfO_2 film on the Si substrate are examined using the well-known X-ray diffraction (XRD) and X-ray photoelectron spectroscopy (XPS) techniques. Second, the forward bias (FB) current-voltage (I-V) properties of MIS SD are investigated at room temperature. The results have demonstrated that these types of structures are suitable for applications in optoelectronic devices.

2. Experimental Details

In this investigation, Si sample pieces measuring 1 cm by 1 cm were taken from an 8″ Si (100) wafer that had a thickness of 600 µm. An HfO_2 interlayer acts as an insulating layer to create n-Si-based SDs. Before deposition, the RAC method was applied to a regular, clean n-Si wafer with a resistivity of 1–10 Ω cm [40]. Native oxides were eliminated using an $HF:H_2O$ (1:10) solution, which was followed by a deionized water rinse. Thermal evaporation was utilised to create an Al metallization with a 60 nm thickness on the rear (rough) side of the cleaned substrate (Si), which was then annealed in a quick thermal processing furnace at 300 °C for 10 minutes in N_2 gas to provide a suitable ohmic contact. Then, quartz glass and n-Si (smooth side) substrates were then coated with a thin layer of HfO_2 using RF-magnetron sputtering. Using a 50 mm diameter, 99.9% pure HfO_2 target, and argon as the sputter gas, four samples of HfO_2/Si diodes were fabricated. The target was pre-sputtered for 10 minutes in an Ar gas atmosphere to eliminate any surface contaminants. Finally, a top metal electrode made of Mo was deposited using direct current sputtering technology in a 1.2 mm 0.3 mm rectangular region with 70 W powers. The electrode has a thickness of 50 nm. The schematic representation of the Mo/HfO_2/Si SD is shown in Figure 1a. The microstructural, elemental, and morphological characteristics of the prepared HfO_2/Si device were analysed using the grazing index X-ray diffraction (GIXRD), X-ray photoelectron spectroscopy (XPS), and field emission scanning electron microscopy

(FESEM). A semiconductor analyzer (Keithley, Model-2636 semiconductor characterisation equipment) was used to conduct the I-V measurements at room temperature.

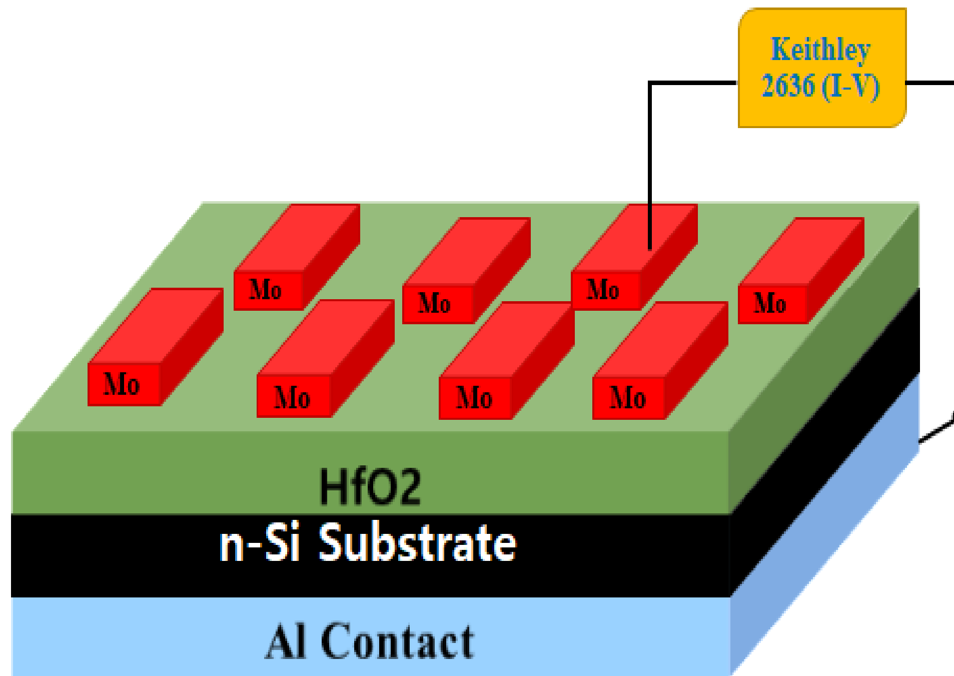

Fig. 1a. The schematic representation of the Mo/HfO_2/Si SD

3. Results and Discussions

The structural characteristics of HfO_2 film on n-Si were examined using XRD, as shown in Fig.1b. It was revealed that the existence of characteristic peaks of HfO_2 film. The characteristics peaks are observed at 17.47^o, 24.42^o, 28.25^o, 31.65^o, 34.53^o, 38.80^o, 45.21^o, 50.72^o, 56.24^o, 60.64^o and 66.02^o for (100), (110), (002), (111), (020), (220), (211), (200), (130), (131) and (023), respectively. The HfO_2 thin film was subjected to XPS survey scans, and the typical wide survey HfO_2 thin film is shown in Fig.1b. The characteristic peaks of Hf (4f, 5p, 4d, 4p), O 1s, and O KLL (Auger peaks) are observed in the general survey spectra. Within the sensitivity of the equipment expecting the adsorbed ambient carbon, none of the contaminating species had been seen [21, 22]. The image from SEM displays that the deposited HfO_2 thin film had a uniform appearance good smoothness of the surface.

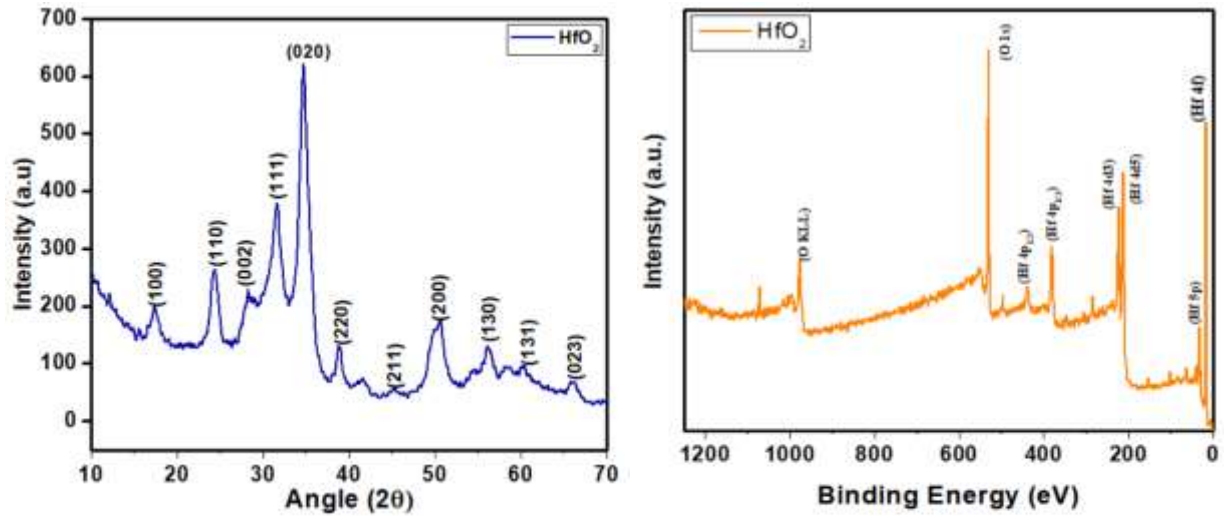

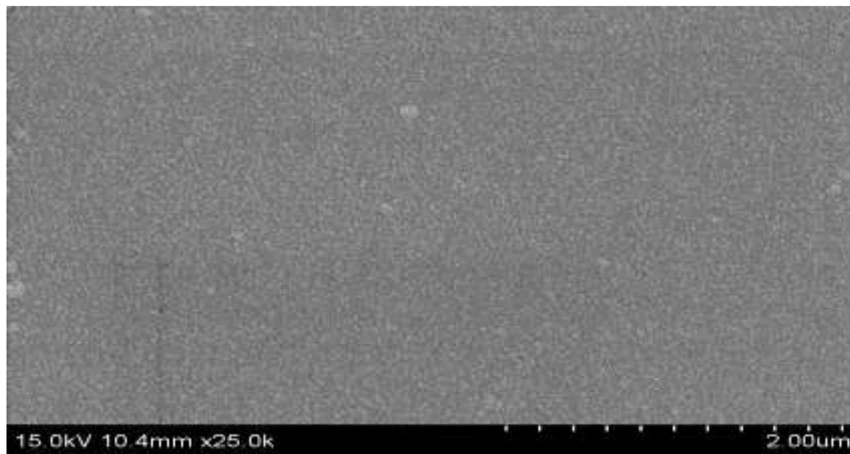

Fig.1b. XRD,XPS plots and SEM image of Mo/HfO_2/n-Si MIS SD

The HfO_2 interlayer is used in the fabrication of the Mo/HfO_2/n-Si MIS SD and evaluates their electrical properties. By using I-V measurements, the electrical characteristic of fabricated MIS SD is investigated. The experimental semi-logarithmic forward and reverse biased current-voltage (I-V) characteristics of Mo/HfO_2/n-Si MIS SD measured in the voltage range from -3V to +3V at room temperature presented in Fig. 2. Specifically, it is observed that the MIS diode shows low leakage current (1.53×10^{-6} A) at -1V. This implies that the HfO_2 as interlayer in between the metal and semiconductor influences the electrical properties of MIS diode. The current through the Schottky barrier diode with the series resistance (RS) and an interfacial layer at a forward bias (V3kT/q), according to the thermionic emission (TE) theory, is given by the relation [23].

$$I = I_0 \exp\left[\frac{q(V-IR_S)}{nkT}\right]\left\{1-\exp\left[\frac{q(V-IR_S)}{kT}\right]\right\} \quad (1)$$

where V, IR_S, q, k, T, n, and I_0, A, A^*, and Φ_b have usual meanings [13, 14]. The reverse saturation current (I_0) is obtained from the intercept of the plot of ln I versus V at V = 0, given by

$$I_0 = AA^* T^2 \exp\left(-\frac{q\Phi_b}{kT}\right) \quad (2)$$

Once the saturation current I_0 has been determined, the Φ_b can be evaluated using the expression

$$\Phi_b = \frac{kT}{q} \ln\left(\frac{AA^*T^2}{I_0}\right) \quad (3)$$

The ideality factor (n) is measure of the conformity of the diode to pure TE, it is determined from the slope of the linear region of forward bias ln I-V using the relation

$$n = \frac{q}{kT}\left(\frac{dV}{d(\ln I)}\right) \quad (4)$$

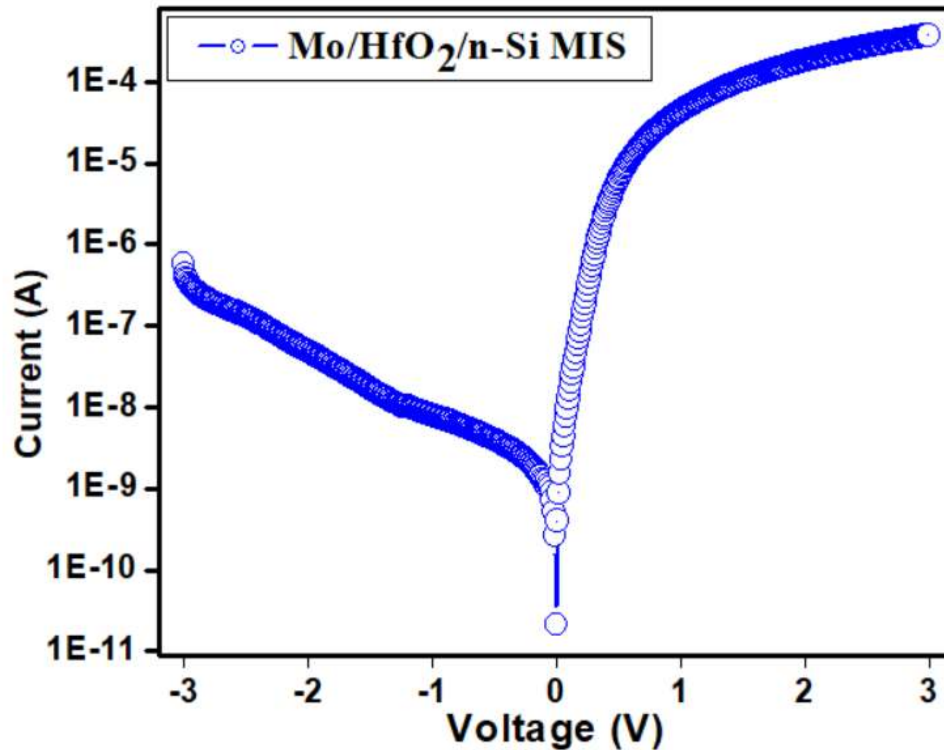

Fig. 2 Forward and reverse ln (*I*)–*V* characteristics of Mo/HfO_2/n-Si MIS SD measured at room temperature in the voltage range ± 3 V.

The Φ_b and n are measured to be 0.82 eV and 1.21 for the SD. Analysis demonstrates that the increased barrier height is caused by a rise in the negative charges at the interface. Electron traps that are localised close to the GaN contact may be to blame for this [25]. It follows that the changing Φ_b is probably the product of changed interfacial chemistry. The various current transport methods, interfacial flaws, and inhomogeneities in the interface may be to blame for the evaluated n value of MIS diode's bigger than unity value [26]. For the higher n values, additional causes could include interface inhomogeneity, non-uniform interfacial charge distribution, the occurrence of surplus current, and recombination current caused by the interface states at the diode [27]. The deviation of the n from unity may be caused by the formation of an electric interlayer at the HfO_2/n-Si interface [28].

The R_S is significant in the region of the non-linear curve in the forward bias I-V characteristics at the high applied voltage. Cheung and Cheung approach [29] also allows for the evaluation of key factors like "n" and R_S. The Cheung's function can be expressed as

$$\frac{dV}{d(\ln I)} = \frac{nkT}{q} + IR_S \tag{5}$$

$$H(I) = V - \left(\frac{nkT}{q}\right) \ln\left(\frac{I}{AA^{**}T^2}\right) \tag{6}$$

H (I) is given as follows:

$$H(I) = n\Phi_b + IR_S \tag{7}$$

The dV/d(ln I) versus I curve for Mo/HfO_2/n-Si MIS SD is illustrated in Fig. 3. The forward bias I-V characteristics' non-linear portion of the plot should result in a straight line. According to Fig. 3, the slope and intercept of the plot are used to derive the 'R_S' and 'n' values. The extracted R_S and 'n' values for Mo/HfO_2/n-Si MIS SD are 1000 Ω and 2.30, respectively. The H (I) - I plot for Mo/HfO_2/n-Si MIS SD at 300 K is also shown in Fig. 3. Eq. (6) states that Fig. 3 is similarly a straight line with an intercept (y-axis) equal to Φ_b results. Φ_b and R_S were determined to be at 0.88 eV and 120 Ω, respectively. The H (I)

against I plot's R_S values match those from the dV/d(ln I) plot, indicating the validity of Cheung's technique.

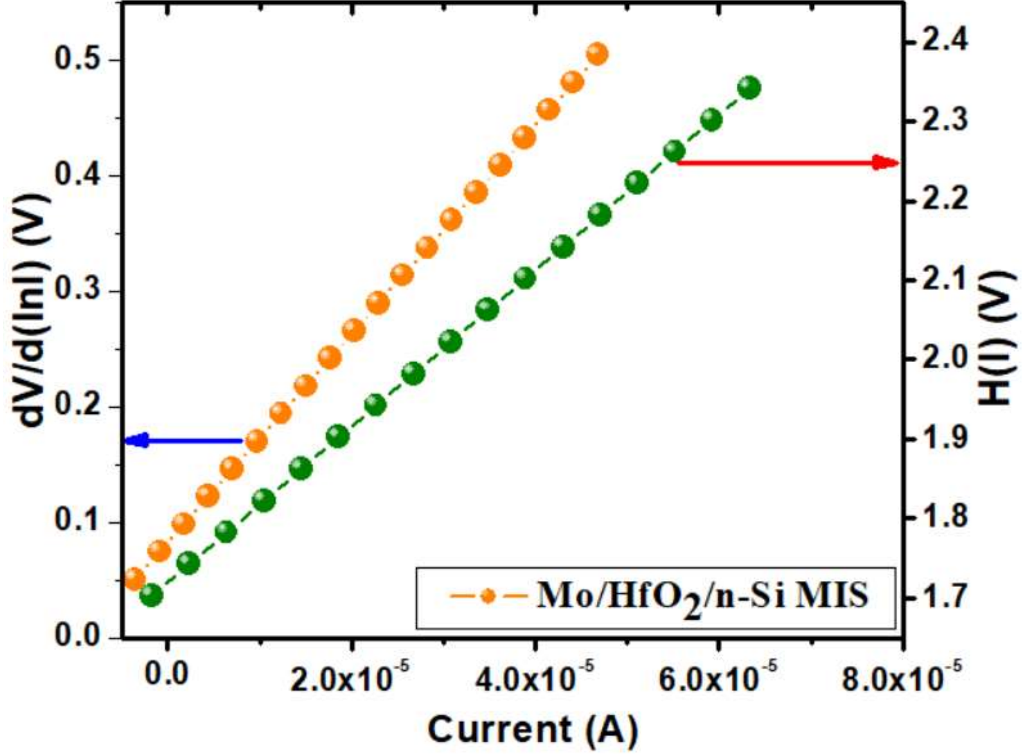

Fig. 3. Plot of dV/dln (I) and H (I) versus I for the Mo/HfO_2/n-Si MIS SD

In order to calculate the effective Φ_b of non-ideal SDs with little leakage current, Hernandez [30] suggested a novel approach. This approach is based on the idea that the Φ_b and n values are variables that depend on voltage. The expression for the voltage-dependent Z(V, T) functions is

$$Z\,(V,T)_i = \frac{kT}{q}\ln\left(\frac{I_i}{AA^*T^2[1-\exp(-qV_d/kT)]}\right) \quad (8)$$

$$Z(V,T)_i = -\Phi_b\,(V,T)_i + \frac{V_d}{n(V,T)_i} \quad (9)$$

where V_d is the diode voltage. The Z(V)-V_d plot is obtained from the linear region I-V characteristics using eq. (8). Fig. 4 shows the plot of $Z(V,T)_i$ versus V_d for the Mo/HfO_2/n-Si MIS diode. If $Z(V,T)_i$ varies linearly with V_d in the i-th voltage interval, then $n(V,T)_i$ and $\Phi_b(V,T)_i$ are quantities and can be found from the intercept and slope, respectively. The values of $\Phi_b(V,T)_i$ and $n(V,T)_i$ have been found as 0.89 eV, 1.2 for MIS diode, respectively.

As can be observed, the values of the Φ_b and ideality factor derived from the Z(V)-V_d plot and the traditional forward bias I-V approach are comparable to one another. Norde and Bohlin proposed a different methodology to determine the Mo/HfO_2/n-Si MIS SD's consistent Φ_b and R_S values [27, 28]. Typically, the n values range from 1 to 2, and the function F (V) can be written as

$$F(V) = \frac{V}{\gamma} - \frac{kT}{q}\ln\left(\frac{I(V)}{AA^*T^2}\right) \quad (10)$$

where I(V) is current obtained from the I-V experimental data, γ is the dimensionless arbitrary integer greater than the value of the n obtained from ln(I)-V characteristics.

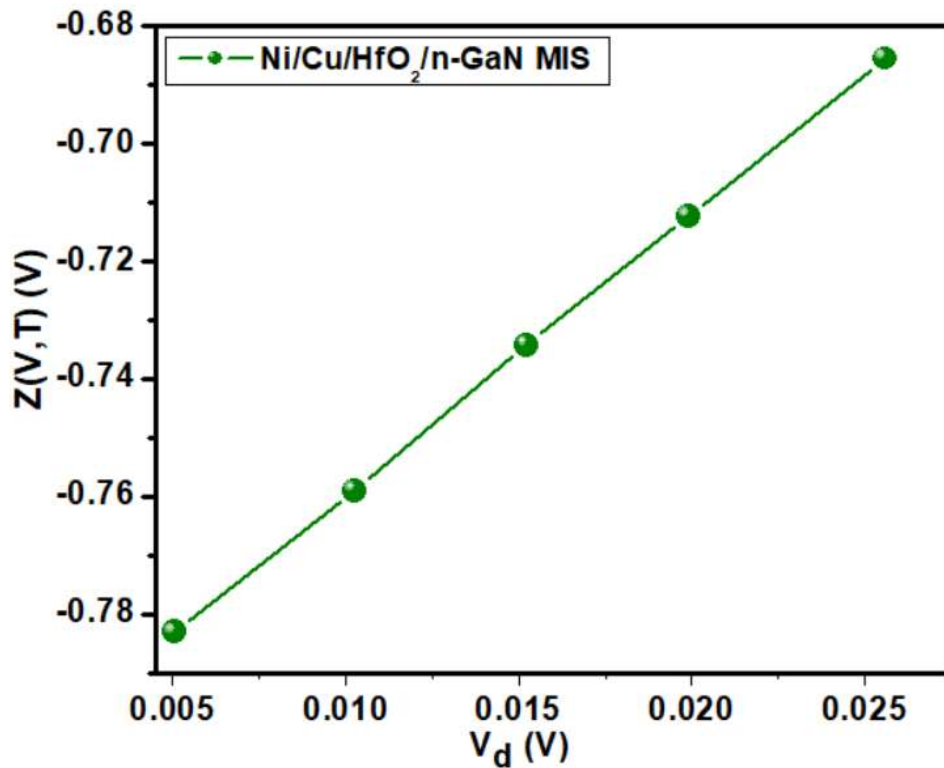

Fig. 4. Plot of Z(V,T) versus V_d for the Mo/HfO_2/n-Si MIS SD

Once the minimum of the F(V) versus V plot is determined, the value of BH can be calculated as

$$\Phi_b = F(V_0) + \frac{V_0}{\gamma} - \frac{kT}{q} \quad (11)$$

where $F(V_0)$ is the minimum point of F(V) and V_0 is the corresponding voltage. Fig. 5 shows the F(V)-V plot of the Mo/HfO_2/n-Si MIS diode. From Norde's function, the value of R_S value can be determined as follows

$$R_S = \frac{kT(\gamma - n)}{qI_0} \tag{12}$$

where I_0 is the corresponding current at the minimum point of $F(V_0)$. The Φ_b and R_S values are extracted from Norde plot, were found to be 0.89 eV and 2998 kΩ for MIS diode.

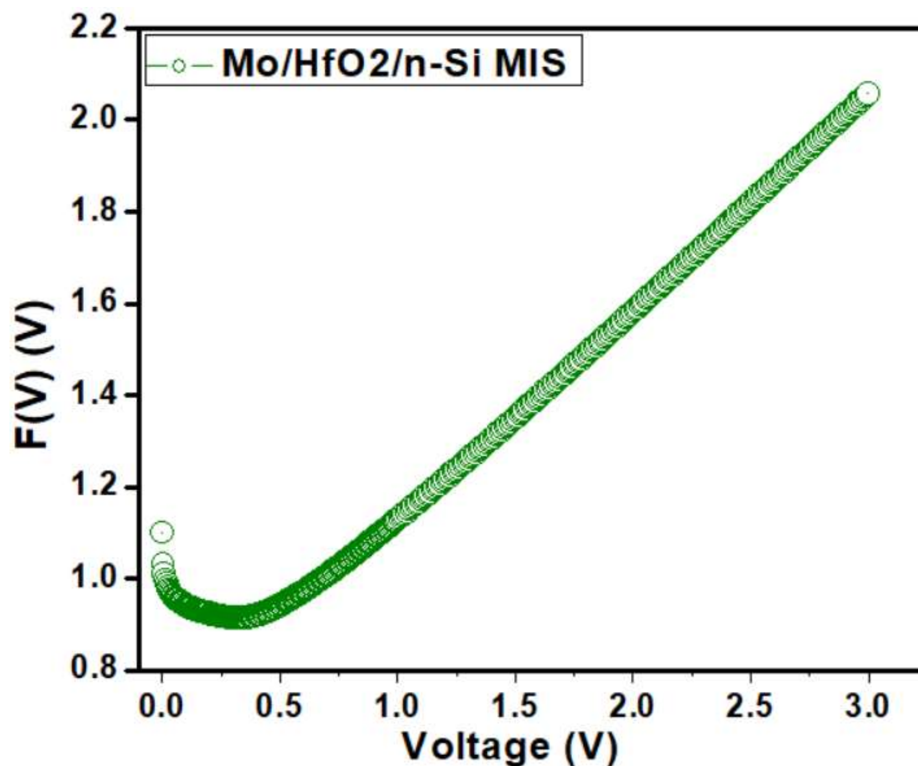

Fig. 5. The Norde plot for the Mo/HfO_2/n-Si MIS SD

According to analysis, there is a little difference between the Φ_b values obtained from the forward bias ln(I)-V, Cheung's, and Norde functions. This difference may be explained by the forward bias ln(I)-V characteristics being extracted from different locations. However, the R_S values obtained from the Norde function is higher than that obtained from the Cheung's functions. Cheung's functions are only applied to the nonlinear region in high voltage section of the forward bias ln(I)-V characteristics, while Norde's function is applied to the full

forward bias region of the ln(I)-V characteristics of the diode. As a result, the approaches used here are trustworthy and efficient.

Fig. 6 shows the forward-biased Mo/HfO_2/n-Si MIS diode's current transport mechanism (CTM). Different linear areas (I, II, and III) with three different slopes are depicted in the log (I) versus log (V) plot. The calculated slope value for Region-I is 1.1, which is quite close to unity and indicates ohmic behaviour. The cause of this could be thermally generated dopants and/or carriers [29].

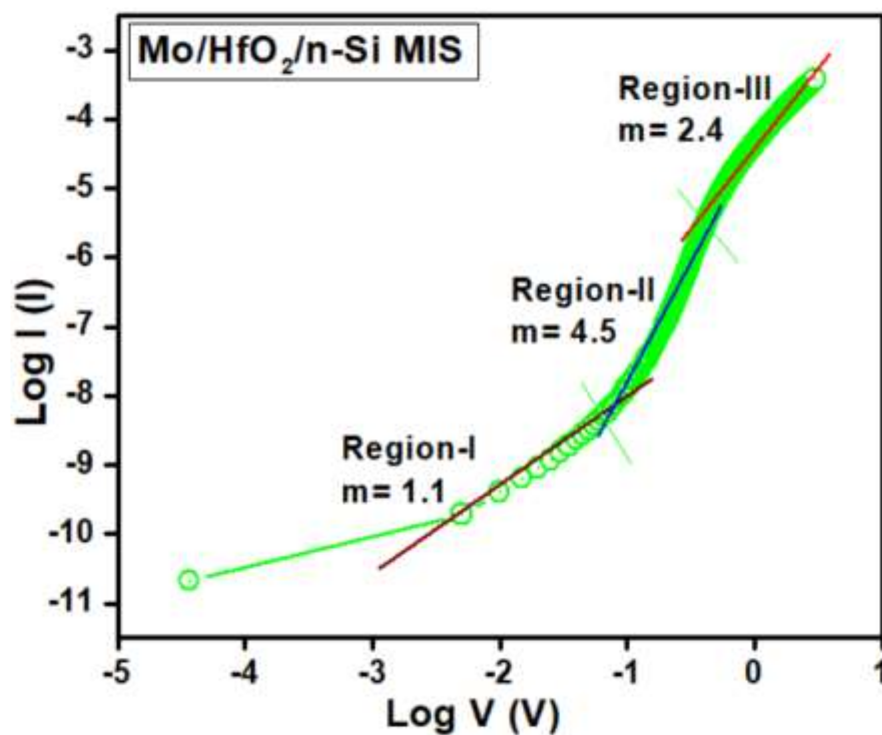

Fig. 6. The forward bias log (*I*) versus log (*V*) plot for the Mo/HfO_2/n-Si MIS diode.

The existence of isolated trapping levels in the Si layer and the high-k HfO_2 layer, which resulted in an estimated slope value in region II of 4.5, which is higher than 2, may be attributed to the space-charge-limited current (SCLC). The value of slope reduces to 2.4 when fitting was done in region-III, suggesting that the developed MIS SD has reached the trap-filling limit [30–32]. According to this research, there is a distinct transition in the carrier transport mechanism at the Mo/HfO_2/n-Si MIS diode interfaces as a function of applied voltage.

In order to understand the current conduction mechanisms at work in the extracted reverse-bias I-V characteristics of the developed Mo/HfO_2/n-Si MIS diode, an ln (I_R) versus $V_R^{1/2}$ plot was drawn and is displayed in Fig. 7. This plot enables one to determine if the extracted reverse-bias I-V curves of the manufactured device exhibit Poole-Frenkel emission (PFE) or Schottky emission (SE) conduction mechanisms.

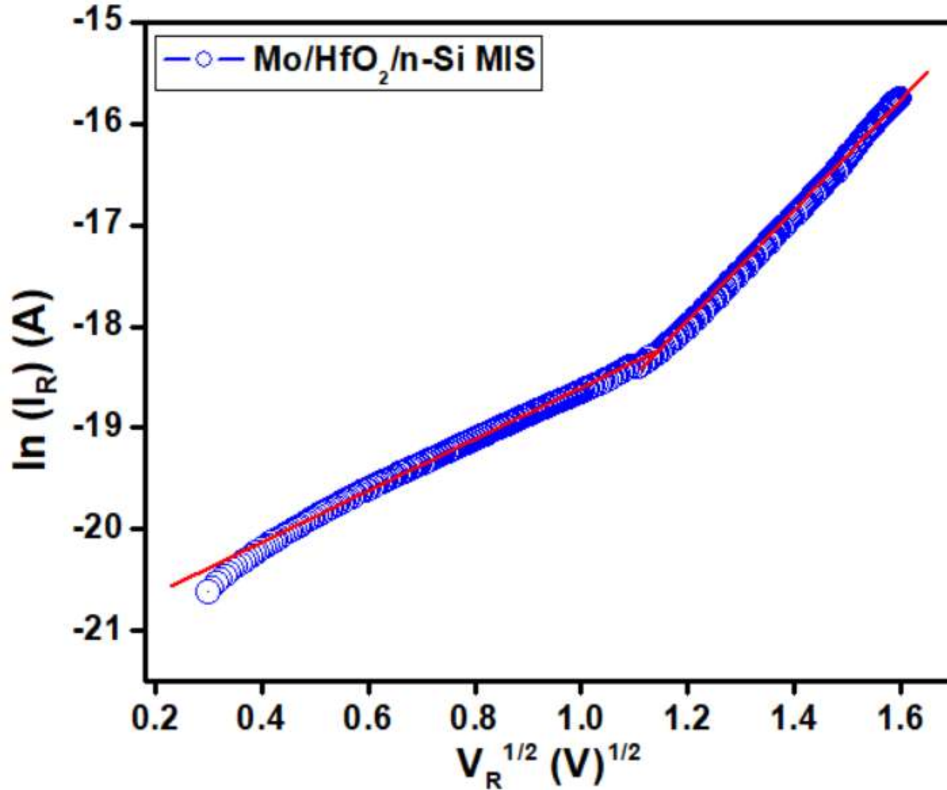

Fig. 7. Plot of ln (I_R) versus $V^{1/2}$ for the Mo/HfO_2/n-Si MIS diode

If the PFE mechanism dominates the current in the reverse bias, it is written as [33].

$$I_R = I_0 \exp\left(\frac{\beta_{PF} V^{1/2}}{kTd^{1/2}}\right) \tag{13}$$

For the Schottky emission (SE) mechanism is defined as

$$I_R = AA^* T^2 \exp\left(-\frac{\Phi_b}{kT}\right) \exp\left(\frac{\beta_{SC} V^{1/2}}{kTd^{1/2}}\right) \tag{14}$$

where "d" represents the film's thickness and "β_{PF} " and "β_{SC}" have their conventional meanings [34]. The following expression can be used to obtain the theoretical values of β_{PF} and β_{SC}:

$$2\beta_{SC} = \beta_{PF} = \left(\frac{q^3}{\pi\varepsilon_0\varepsilon_r}\right)^{1/2} \quad (15)$$

β_{PF} is always twice that of β_{SC}. However, in the case the MIS diode exhibit two distinct regions observed (Fig. 7) that show the two different conduction mechanisms that occur in the reverse bias. The extracted slope values are 5.26×10^{-5} $eVm^{1/2}V^{-1/2}$ in the lower bias region (region I) and 1.31×10^{-5} $eVm^{1/2}V^{-1/2}$ in the higher bias region (region II) for the MIS SD. It is discovered that the retrieved slope value in region I closely resembles the theoretical value of the Poole-Frenkel lowering coefficients. Therefore, the Poole-Frenkel emission in region I dominates the reverse leakage current conduction mechanism. This suggests that rather than emitting directly from the metal, carriers are transported from it into conductive dislocations through trap states [35, 36]. The recovered slope value in area II, however, comes quite close to matching the theoretical value of the Schottky lowering coefficients. This shows that in region II, where current conduction occurs through the interface rather than from bulk material, the Schottky emission is the predominant current conduction mechanism. This is caused by the dielectric layer used here, which has an irregular and subatomic structure [37–40].

Conclusions

In summary, the HfO_2 thin film was deposited on n-Si semiconductor by using radio frequency (RF) magnetron deposition technique. The structural and surface morphological properties of HfO_2/n-Si interface have been explored by XRD and XPS techniques. To study the electrical properties of fabricated Mo/HfO_2/n-Si MIS diode, I-V measurements are used at room temperature. Experimental results show that the MIS diode shows a good rectifying behavior, lower leakage current. The evaluated Φ_b of the MIS diode is very high. The enhancement of the Φ_b attributed to the fact that the HfO_2 interlayers enhances the effective Φ_b by influencing the depletion region of n-Si. Several methods have been used to extract

diode parameters, such as Φ_b, n and Rs from the experimentally obtained I-V characteristics. Steadiness in the extracted values using dissimilar methods was observed. From the forward-bias *I–V* curves of Mo/HfO_2/n-Si MIS diode, Ohmic and SCLC conduction pathways are discovered to be active in the low-voltage and high-voltage regimes, respectively. The lower and greater bias areas' predominant current conduction mechanisms are Poole-Frenkel and Schottky emissions, according to reverse I-V characteristics. In conclusion, it was determined that the intentionally deposited HfO_2 and undoped GaN buffer layers in the manufactured Mo/HfO_2/n-Si MIS diode were responsible for the improvements in the rectification ratio, SBHs, and satisfactory fitting of experimental data to equations of various methodologies. As a result, the findings of our study are valuable for formulating a manufacturing plan and producing high-performance n-Si-based MIS devices.

References:

[1]. Y. Atasoy, M.A. Olgar, E. Bacaksiz, J. Mater. Sci. 30, 10435–10442 (2019)

[2]. F.A. Mir, S. Rehman, K. Asokan, S.H. Khan, G.M. Bha, J. Mater. Sci. 25, 1258–1263 (2014).

[3]. H.H. Gullu, D.E. Yildiz, J. Mater. Sci. 30, 19383–19393 (2019).

[4]. J.B. Park, W.S. Lim, B.J. Park, I.H. Park, Y.W. Kim, G.Y. Yeom, J. Phys. D Appl. Phys. 42, 055202 (2009)

[5]. C. Buttay, H.-Y. Wong, B. Wang, M. Xiao, C. Dimarino, Y. Zhang, Microelectron. Reliab. 114, 113743 (2020).

[6]. G. He, L.Q. Zhu, M. Liu, Q. Fang, L.D. Zhang, Appl. Surf.Sci. 253, 3413 (2007).

[7]. S.Y. Lee, S. Chang, J.S. Lee, Thin Solid Films 518, 3030(2010)..

[8]. M.H. Al-Dharob, A. Kokce, D.A. Aldemir, A.F. Ozdemir, S. Altındal, J. Phys. Chem. Solids 144, 10952 (2020).

[9]. C. Liu, E. F. Chor, L. S. Tan, Appl. Phys. Lett. 88 (2006) 173504(1-3).

[10]. K. Cico, J. Kuzmik, D. Gregusova, R. Stoklas, T. Lalinsky, A. Georgakilas, D. Pogany, K. Frohlich, Microelectron. Reliab. 47 (2007) 790-793.

[11]. S. Kim, Y. Hori, W.-C. Ma, D. Kikuta, T. Narita, H. Iguchi, T. Uesugi, T. Kachi, T. Hashizume, Jpn. J. Appl. Phys. 51 (2012) 060201(1-3).

[12]. A. Shetty, B. Roul, S. Mukundan, L. Mohan, G. Chandan, K. J. Vinoy, S. B. Krupanidhi, AIP Advances 5 (2015) 097103(1-11).

[13]. V. Manjunath, V. Rajagopal Reddy, P.R. Sekhar Reddy, V. Janardhanam, Chel-Jong Choi, Curr. Appl. Phys. 17 (2017) 980-988.

[14]. C. Venkata Prasad, M. Siva Pratap Reddy, V. Rajagopal Reddy, Chinho Park, Appl. Surf. Sci. 427 (2018) 670-677.

[15]. H.-I. Chen, C.-H. Chang, H.-H. Lu, I-P. Liu, W.-C. Chen, B.-Y. Ke, W.-C. Liu, Sens. Actuators B: Chem. 262 (2018) 852-859.

[16]. A. Vinod, M. Singh Rathore, N. Srinivasa Rao, Vacuum 155,339–344 (2018).

[17]. P.R. Sekhar Reddy, V. Janardhanam, K.-H. Shim, V. Rajagopal Reddy, S.-N. Lee, S.-J. Park, C.-J. Choi, Vacuum 171, 109012 (2020).

[18]. I. Karaduman, O. Barın, M. Ozer, S. Acar, J. Electr. Mater.45, 8 (2016).

[19]. P. Harishsenthil, J. Chandrasekaran, R. Marnadu, P. Balraju,C. Mahendarn, Physica B 594, 412336 (2020).

[20]. I.R. Kaufmann, A. Pick, M.B. Pereira, H. Boudinov, Thin Solid Films 621, 184–187 (2017).

[21]. A. K. Mondal, L. K. Ping, M. A. S. M. Haniff, M. A. M. Sarjidan, B. T. Goh, M. A. Mohamed, ACS Omega 7 (2022) 2252-2259.

[22]. X. Luo, Y. Li, H. Yang, Y. Liang, K. He, W. Sun, H.-H. Lin, S. Yao, X. Lu, L. Wan, Z. Feng, Crystals 8 (2018) 248(1-16).

[23]. E. H. Rhoderick and R. H. Williams: Metal-Semiconductor Contacts, 2nd ed.,

(Oxford, Clarendon press, 1988) p. 33.

[24]. V. Rajagopal Reddy, V. Janardhanam, Jin-Woo Ju, Hyobong Hong, Chel-Jong Choi, Semicond. Sci. Technol. 29 (2014) 075001(6pp).

[25]. V. Rajagopal Reddy, V. Janardhanam, Jin-Woo Ju, Hyobong Hong, Chel-Jong Choi, Semicond. Sci. Technol. 29 (2014) 075001(6pp).

[26]. M. Saglam, A. Ates, B. Guzeldir, A. Astam, M.A. Yildirım, J. Alloy. Compd. 484 (2009) 570-574.

[27]. R. T. Tung, Phys. Rev. B 45 (1992) 13509-13523.

[28]. A. Kumar, M. Heilmann, M. Latzel, R. Kapoor, I. Sharma, M. Gobelt, S. H. Christiansen, V. Kumar, R. Singh, Sci. Rep. 6 (2016) 27553(1-11).

[29]. S. Kumar, M.V. Kumar, S. Krishnaveni, Semicond 54, 169 (2020).

[30]. K. Ashish, V. Seema, R. Singh, J. Nano-Electron. Phys. **3**, 671 (2011).

[31]. C. Venkata Prasad, V. Rajagopal Reddy, Chel-Jong Choi, Appl. Phys. A 123 (2017) 279(1-10).

[32]. Y.S. Ocak, M. Kulakci, T. Kılıcoglu, R. Turan, K. Akkılıc, Synth. Met. **159**, 1603 (2009).

[33]. A.A. Kumar, V.R. Reddy, V. Janardhanam, H.D. Yang, H.-J. Yun, C.J. Choi, J. Alloys Compd. 549, 18 (2013).

[34]. P. R. Sekhar Reddy, V. Janardhanam, V. Rajagopal Reddy, Min Hyuk Park, · Chel-Jong Choi, Applied Physics A (2021) 127:803.

[35]. V.R. Reddy, V. Manjunath, V. Janardhanam, Y.-H. Kil, C.-J. Choi, J. Electron. Mater. 43, 3499 (2014).

[36]. K. Akkılıc, Y.S. Ocak, T. Kılıcoglu, S. Ilhan, H. Temel, Curr. Appl. Phys. 10, 337 (2010).

[37]. I. Rahim, M. Shah, M. Iqbal, F. Wahab, A. Khan, S.H. Khan, Phys. B 524, 97

(2017).

[38]. A. Tataroglu, Chin. Phys B. 22, 068402 (2013).

[39]. S. Altındal Yerişkin, J Mater Sci: Mater Electron. 30 (2019).

[40]. A. Buyukbas-Ulusan, S. Altındal-Yerişkin, A. Tataroğlu, J. Mater. Sci. Mater. Electron. 29 (2018).